Project Final Report

Interdisciplinary Assessment of Mercury Transport, Fate and Risk in Enid Lake, Mississippi

Principal investigators:

PI: Dr. Xiaobo Chao, Senior Research Scientist, National Center for Computational Hydroscience and Engineering (NCCHE), The University of Mississippi (UM), chao@ncche.olemiss.edu, 662-915-8964

Co-PI: Dr. James V. Cizdziel, Assistant Professor, Department of Chemistry and Biochemistry, UM, cizdziel@olemiss.edu,

Co-PI: Dr. Kristie Willett, Associate Professor, Department of Pharmacology, UM , kwillett@olemiss.edu

Co-PI: Dr. A.K.M. Azad Hossain, Research Scientist, NCCHE, UM, ahossain@ncche.olemiss.edu

Cooperators: ARS, National Sedimentation Laboratory, Oxford, MS
              Mississippi Department of Environmental Quality, Jackson, MS

Abstract

Enid Lake is one of the important large recreation lakes in Mississippi, and the mercury level is relatively high compared with other large lakes. This research brought together a team of scientists that with their expertise in analytical chemistry, remote sensing technology, hydraulic modeling and risk assessment to study the transport, fate and risks of mercury in Enid Lake. Two field measurements were conducted in spring and fall to measure the flow, sediment and mercury in Enid Lake. The remote sensing technology was applied to analyze the concentration distributions of sediment and mercury in the whole lake, and the results are generally in good agreement with measured data. A numerical model was developed to simulate the flow, sediment, and mercury in the lake, and the interaction between the mercury and sediment was taken into accounted. Risk assessment was conducted to analyze the potential risk of mercury both in the environment and human fish consumption. The research results help us understand the transport mechanisms of sediment and mercury in large lakes, and provide useful information for decision makers to evaluate established TMDLs and fish consumption advisories.

INTRODUCTION

The Yazoo River Basin is the largest basin in Mississippi. Abundant streams, reservoirs and lakes are located in this region, including four large flood control reservoirs: Arkabutla Lake, Sardis Lake, Enid Lake and Grenada Lake. These lakes are significant natural and recreational resources. The soils in this region are highly erodible, resulting in a large amount of sediment discharged into water bodies. Understanding the dynamic processes of contaminated sediment movement and fate and transport of pollutants in these large recreation lakes is important to manage the water quality of the lakes and provide useful information for fish consumption advisories and potential risk assessment. The processes of contaminated sediment transport and settling in the lake are particularly critical to lake water quality because of associations between sediment and other pollutants (nutrients, PCBs, mercury, etc.).

Mississippi Department of Environmental Quality (MDEQ 2010, 2012) reports that many water bodies in this region are impaired due to contaminated sediment, and nutrients, suspended sediment (SS), DDT, PCBs, pathogens, and mercury have been identified as major pollutants. Since 1995, Enid Lake has been listed among now 14 water bodies that are under fish consumption advisories for mercury in Mississippi, reducing the recreation values of these lakes. In 2002 a Total Maximum Daily Loads (TMDLs) was developed for mercury in the Yocona River including the Enid Lake. The MDEQ adopted a criteria of 12 ng/L to protect aquatic life with a margin of safety of 50% (MDEQ 2002). Unfortunately, most of the fish and sediment data available to regulators is more than 10 years old (MDEQ 2002, Huggett et al. 2001).

Mercury is a widely distributed and persistent pollutant in the environment. The chemical forms of mercury in air, water, and sediment include elemental mercury Hg(0), inorganic ionic mercury (HgII), and the organic form methylmercury (MeHg). When mercury enters the water and soil, microorganisms transform the mercury into MeHg, which is the most toxic form and accumulated by fish, shellfish and other aquatic organisms (Selin et al.,2010). When humans consume contaminated fish, they are exposed to mercury. The adverse effects of mercury in humans include neurodevelopmental, cardiovascular, and immunological deficits (Karagas et al.,2012; Grandjean et al.,2010). The Food and Drug Administration action level restricts fish tissue mercury concentrations to less than 1.0 ppm (MDEQ 2002). Largemouth bass, carp, gar, black crappie, and catfish collected from Enid Lake have had concentrations that exceeded the 1 ppm standard (Huggett et al.,2001; MDEQ 2002). In fact, consumption advisories are in place for over 26% of the US river miles and 38% of its total lake acreage (Knightes et al.,2009). Characteristics of particular fish (e.g. growth and consumption rates, type of prey, age and length) impact mercury bioaccumulation (Ward et al.,2010).

Sediment plays an important role in the fate and transport processes of mercury in water bodies. Mercury may adsorb to sediment particles and also desorb from sediment to the water, and a linear approach can be applied to describe the processes of adsorption/desorption (Katsenovich et al 2010). Bed sediment associated mercury can be released gradually into the water column due to diffusion and sediment resuspension (Kuwabara et al 2003). Figure 1 shows the mercury cycle in a water body.
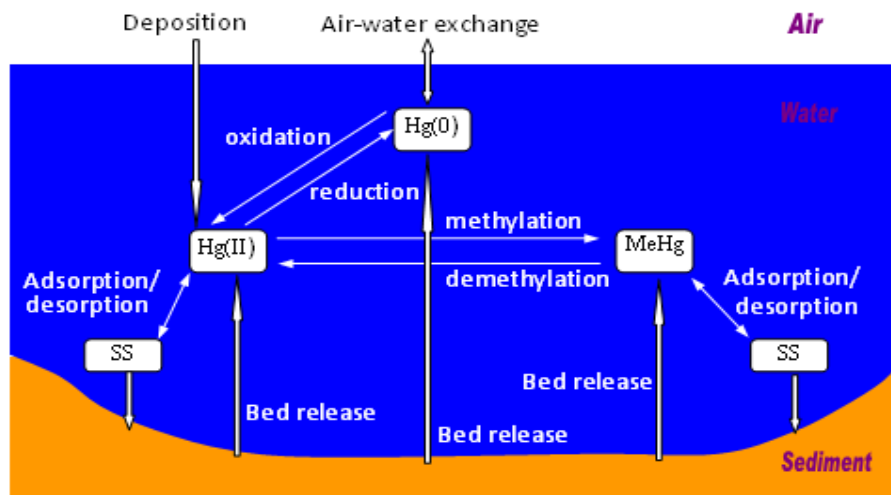

Figure 1. The mercury cycle in a water body

In this project, the concentrations of mercury in water and sediment were measured in spring and fall in Enid Lake. The fate and transport processes of mercury in the lake were studied based on field observation, remote sensing technology, numerical model, and risk assessment. Our research not only updates the fate and transport of mercury in Enid Lake, it is also directly relevant to stakeholders

concerned with wildlife and human consumption of mercury. The measured and computed mercury concentrations in water, sediment, and fish have been used for a potential risk assessment. It has greatly improved our understanding of the transport mechanism of mercury by water and sediments in large lakes of Mississippi and provides more timely data on associated potential risks. It is anticipated that results from this study will be directly applicable to other large lake systems in Mississippi. The results of this research can be used by decision makers to evaluate TMDLs for the watershed feeding into the lake.

OBJECTIVES

The overall goal of this research is to study the transport, fate and risk of mercury in Enid Lake. We have brought together a team of scientists particularly well suited to: provide sensitive field measurements, utilize innovative remote sensing technologies, generate novel numerical mercury fate modeling and provide up-to-date risk assessment. To reach this goal, the following objectives were designed: (1) measurements of flow, sediment and mercury in the lake; (2) application of remote sensing technology to analyze sediment and mercury in the lake; (3) development of a numerical model to simulate the flow, sediment, and mercury distribution in the lake; (4) Assessment of the potential risk of mercury both in the environment and human fish consumption.

RESEARCH METHODS

(1) Study site
Enid Lake is a large reservoir located in Yazoo River Basin, Mississippi (Fig. 2). It is a USACE flood control structure built in 1952. It was impounded by Enid Dam on the Yocona River in Yalobusha County and covers an area of 60 square km. The soils in this region are highly erodible, and the erosion rate has been recognized as one of the highest place in the nation (Bennett and Rhoton 2009). This lake has significant natural and recreational resources. However, it is impaired by mercury, and a fish consumption advisory was issued by MDEQ in 1995. In order to reduce the mercury level in the lake, mercury TMDL has been established in the lake watershed (MDEQ 2002). The proposed research is to study the transport processes of sediment and mercury, and their interactions in water bodies based on field measurement, numerical model and remote sensing technique.
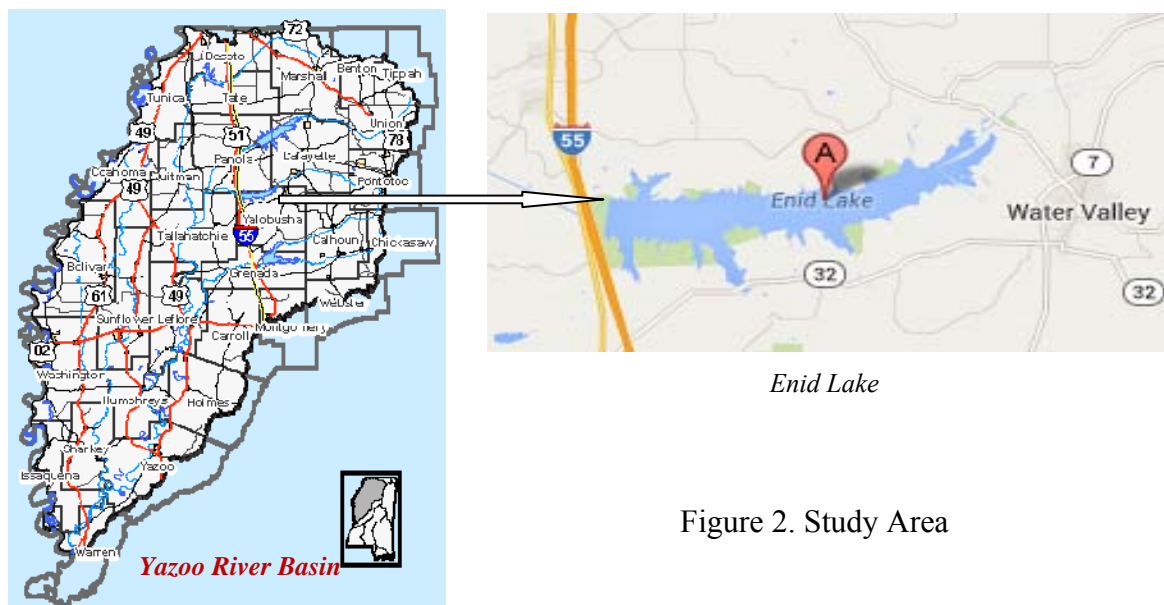

Yazoo River Basin

Enid Lake

Figure 2. Study Area

3

## (2) Field sampling and measurements in Enid Lake

The observed flow discharges in Yocona River, and the water level data in Enid Lake can be obtained from USGS and USACE. Some bed sediment and mercury concentration in water, sediment and fish previously measured by the University of Mississippi (UM), NSL and MDEQ were used in this study (Huggett et al 2001, Bennett and Rhoton 2009). Additional field measurements were conducted in the lake to measure flow velocity, water level, suspended sediment (SS) concentration and mercury concentration in water and sediment. In this project, two field measurements were conducted on March 12 and Nov. 19, 2013. Figure 3 shows the sampling locations in the lake.

a. Flow measurements

Velocity profiles, water depth and water surface elevations at different locations (shown in Fig.3b) of the lake were measured using Acoustic Doppler Current Profiler (ADCP) by scientists at NSL. At each location (Fig. 3), the coordinates were identified using GPS, and the concentrations of SS were determined for select samples using a portable SS meter from Insite IG Inc.

b. Water sampling

Water and sediment samples were collected at each location (Fig.3). The collected samples were used to measure the SS concentration, total mercury concentration in water, and sediment.
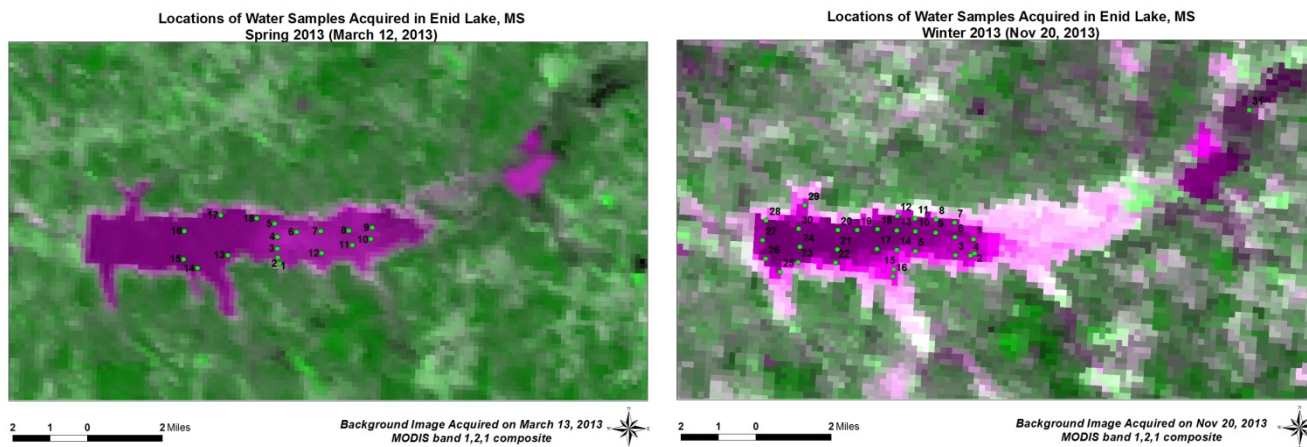
a. Sampling locations on March 12, 2013   b. Sampling location on Nov. 19, 2013

Figure 3. Sampling locations in the lake

c. Fish sampling

Electro-shocking is a non-lethal survey method used to temporarily paralyze the fish so they can easily be collected. The fish collected from Enid Lake were of species commonly sought after and consumed by local fishermen. The fish samples with three different species, Crappie (CR), Largemouth Bass (LMB) and Channel Catfish (CC), were collected by the USDA National Sediment Laboratory (NSL).

(3) Laboratory measurements

a. Total mercury in sediments

The sampled sediment was analyzed for total mercury using automatic mercury analyzer (DMA-80; Milestone Inc., Shelton, CT) which was based on thermal decomposition (TD), amalgamation,

and atomic absorption spectrometry (AAS). The approach follows US EPA Method 7473. About 0.25 g of sediment samples are weighed directly into nickel combustion boats. The boats are automatically inserted into the instrument where the samples are dried and combusted in oxygen releasing Hg vapor. The combustion products are swept through a catalyst tube where oxidation is completed, and halogens, nitrogen and sulfur oxides (which can interfere with the analysis) are trapped. The remaining gases are carried to the gold amalgamator which traps Hg. The system is flushed with oxygen to remove decomposition products. The amalgamator is then rapidly heated releasing Hg vapor into two absorbance cells which are positioned in the light path of a single wavelength AAS. Absorbance is measured at 253.7 nm as a function of Hg concentration. The instrument was calibrated using a sediment reference material (e.g. MESS-3). Another reference material (e.g. SRM 1573a) was analyzed every 10 samples for a QC check. The values obtained were deemed acceptable if they were within 15% of the certified value. During each run a subset of samples were analyzed in duplicate. The relative percent difference was less than 15%. Blanks were also run every 10 samples. The amount of Hg for the blanks were negligible (<0.1 ng); this corresponded to a concentration of ~ 0.40 ng/g using the typical weight of analyzed sample (0.25 g).

b. Total mercury in water

Total-Hg in water samples was determined using CVAFS following EPA Method 1631. Water samples were filtered and both filtered and unfiltered fractions measured. Water was passed through a pre-heated (~500°C) glass-fiber filter. The samples were preserved using ultrapure HCl or BrCl as described in the EPA method and holding times were observed. The glass fiber filter was also analyzed for particulate mercury.

c. Loss-on-Ignition

Loss on Ignition (LOI) was used to estimate Total Organic Matter. LOI was calculated by reweighing the sample boats after the total-Hg analyses. Temperatures were kept under 440ºC to prevent breakdown of carbonates which would introduce inorganic carbon into the calculation.

$$\%LOI = \frac{\left[\left(sample\ wt.+boat\ wt.\ before\ Hg\ analysis\right)-\left(sample\ wt.+boat\ wt.\ after\ Hg\ analysis\right)\right]}{\left(sample\ wt.+boat\ wt.\ before\ Hg\ analysis\right)-empty\ boat\ weight}\times 100$$

d. Sediment analysis

Total Suspended Solids was determined by passing a known volume of sample (between 150 ml to 500 ml depending on sediment load) through a 0.45 μm quartz wool filter that was combusted prior to filtering to remove any Hg. The filter was allowed to dry at room temperature under a laminar flow hood and reweighed to determine the TSS concentration using the following formula [US EPA Method 160.2]:

TSS (mg/L) = ((Residual + Filter (mg)) - Filter (mg)) / sample filtered (mL)) * 1000 (mg/L)

To determine PBM, the filters were then analyzed by combustion atomic absorption spectrometry using a direct mercury analyzer (DMA-80) following US EPA Method 7473. The instrument was calibrated using a standard solution containing known amounts of Hg. Reference materials including MESS-3 (sediment) and Joaquin Soil were used to as calibration checks every 10 samples; recoveries were between 88 to 115 % of the certified values. Blank filters were run every 10 samples to assure that Hg was not being carried over between samples. The amount of Hg for the blanks was negligible. The method detection limit for the analysis was estimated at 0.2 ng/g. The technique has been thorough discussed in earlier chapters.

For particle size distribution analysis, sediments were homogenized in their container by stirring with a Teflon-coated spatula. A portion of the sediment was transferred to plastic weighing boats and

allowed to air-dry in a clean laminar flow hood. Once dry, the sample was crushed using a clean mortar and pestle and a few grams were set aside for total-Hg analyses. The remaining portion was weighed and placed into a beaker with DI water and sonicated for 1 hour to break up adhering particles. The sample was then wet-sieved through stainless steel meshed screens with openings of 1000 μm, 500 μm, 250 μm, and 125 μm. The screen contents were visually inspected to confirm that there were no clumps; if necessary a spatula was used to further gently break up adhering materials. The screens were then allowed to air-dry and the contents were weighed. Particle size distribution was determined on a weight percent basis. The difference between the initial starting weight and the combined weights of sediment collected on the screens was used for the <125 μm category.

For determination of total-Hg and loss-on-ignition in sediment, total-Hg was measured in the bulk sediment and in each size fraction using a direct mercury analyzer (DMA-80) based on thermal decomposition, amalgamation, and atomic absorption spectrometry following EPA Method 7473. Quality assurance protocols were the same as discussed earlier. To obtain Hg data for the <125 μm fraction, samples were dry sieved and the material passing through the fine mesh was analyzed. Loss-on-ignition (LOI), which is used as an estimate of organic matter, was determined by weighing the boats before and after combustion.

e. Fish mercury analysis

Once collected, the fish were placed on ice and taken to laboratory for analysis. In the laboratory the fish were dissected. The muscle and liver tissues were used for total-Hg analysis, while other organs including gills, gonad, kidney, heart, sperm, and eggs were preserved for use in other analyses. All samples were stored in individual vials and bags and frozen until analyzed (Brown 2013). For the present study, only data for the muscle for crappie, largemouth bass, and channel catfish were used.

(4) Estimation of suspended sediment and mercury concentration using remote sensing technology

SS concentration has been estimated and mapped successfully using remote sensing for the last three decades. Different approaches and algorithms had been developed over time for SS concentration estimation/mapping using optical satellite data. The available techniques can be categorized into four general groups: (1) simple regression (correlation between single band and in-situ measurements)[e.g., Williams and Grabau (1973) – Chesapeake Bay early in 1973], (2) spectral unmixing techniques, (3) Band ratio technique using two and more bands [e.g., Lathrop ,1992; Populus et al., 1995; Wang et al., 2003], and (4) multiple regressions[e.g., Binding et al., 2005].

Hossain et al. (2010) developed a remote sensing based index and determined the co-efficients that can be used in riverine/lake environments quantitative mapping of the SS concentrations. Normalized Difference Suspended Sediment Index (NDSSI) (Eq.1) was calculated using the Landsat data and was correlated to the near real-time in-situ measurements of SS concentrations using a power equation (Eq.4) for quantitative estimation of SS concentration in the Mississippi River.

This technique, using the obtained coefficients was applied to estimate/map the SS concentration in the Mississippi River during the 2008 US Midwest flood and in Lake Pontchartrain during (1) Bonnet Carre Spillway opening event and (2) before and after Hurricane Katrina. The results were compared by the simulation results of CCHE2D (a numerical model developed at NCCHE) and found in a good general agreement qualitatively and quantitatively (Figure 4). The results indicate that (1) NDSSI has the potential to estimate (relative variation) and map the spatial distribution of SS concentration in both river and lake environments, (2) NDSSI can be used for quantitative estimation of SS concentration in these environments when coupled with two coefficients in a power equation, and (3) the same approach can be used to estimate SS concentration in both river and lake water within reasonable error limits using NDSSI.

$$NDSSI = \frac{\rho_B - \rho_{NIR}}{\rho_B + \rho_{NIR}} \qquad\qquad (1)$$

$$SSC = a \times NDSSI^{-b} \qquad\qquad (2)$$

Where, ρ_B and $\rho_{NIR,}$ are the reflectance values of Landsat 5/7 TM/ETM+ Band 1, Band 3 and Band 4 respectively.
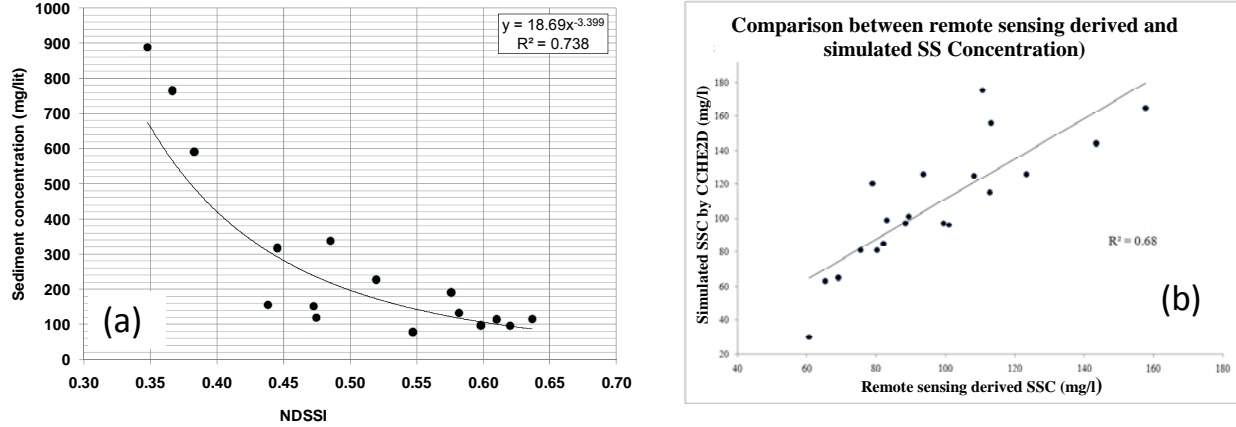

Figure 4. (a) Relationship between NDSSI and in-situ measurements of SS concentrations in water; (b) Quantitative comparison between simulated SS concentration (by CCHE2D) and remote sensing derived SS concentration estimation (By NDSSI) (Hossain et al., 2010).

In Enid Lake, NDSSI was calculated using Landsat TM imagery for different seasons to map the relative variation of suspended sediments. However, due the limitation of cloud coverage and coarse temporal resolution it was not possible to use Landsat TM imagery to quantitative estimation of suspended sediments and associated mercury. MODIS imagery was available after the studied storm events and were used for quantitative estimation of suspended sediments and associated mercury concentration. The MODIS imagery used and corresponding in situ measurements of suspended sediments and mercury concentration are shown in Figure 3. The detail of MODIS based suspended sediments and mercury concentration estimation are discussed in the results section.

(5) Numerical modeling of flow, sediment and mercury in the lake

The National Center for Computational Hydroscience and Engineering (NCCHE) of the University of Mississippi has developed a three-dimensional hydrodynamic and sediment transport model, CCHE3D. This model has been verified against analytical solution, and validated using experimental data and field measurements (Jia et al. 2005, 2009, Wang 2008). Inspired by the success of the CCHE3D model, in recent years, a three-dimensional water quality model, CCHE3D_WQ has been developed for simulating temporal and spatial variations of water quality with respect to phytoplankton, nutrients, dissolved oxygen, suspended sediment and salinity. In this model, the effects of suspended and bed sediment on the water quality processes were considered. It has been applied to studies of sediment, water quality and chemical contamination problems in nature lakes (Chao et al 2006, 2007, 2008).

In this research, a numerical model was developed based on CCHE3D for simulating the fate and transport of mercury in large lakes. Total mercury in water and sediment was simulated, and the processes including advection, diffusion, adsorption/desorption, bed release, settling, etc., were considered in the model. The developed module has been integrated into CCHE3D for simulating flow, sediment, and mercury in Enid Lake.

Flow modeling

The governing equations of continuity and momentum of the three-dimensional unsteady hydrodynamic model can be written as follows:

$$\frac{\partial u_i}{\partial x_i} = 0 \tag{3}$$

$$\frac{\partial u_i}{\partial t} + u_j \frac{\partial u_i}{\partial x_j} = -\frac{1}{\rho}\frac{\partial p}{\partial x_i} + \frac{\partial}{\partial x_j}\left(\nu \frac{\partial u_i}{\partial x_j} - \overline{u_i' u_j'}\right) + f_i \tag{4}$$

where u_i ($i=1,2,3$) are Reynolds-averaged flow velocities (u, v, w) in Cartesian coordinate system (x, y, z); t is the time; ρ is the water density; p is the pressure; ν is the fluid kinematic viscosity; $-\overline{u_i' u_j'}$ is the Reynolds stress; and f_i are body force terms.

The free surface elevation (η_s) is computed using the following equation:

$$\frac{\partial \eta_s}{\partial t} + u_s \frac{\partial \eta_s}{\partial x} + v_s \frac{\partial \eta_s}{\partial y} - w_s = 0 \tag{5}$$

where u_s, v_s and w_s are surface velocities in x, y and z directions; η_s is the water surface elevation.

Wind stress is one of the most important driving forces for lake water movement. The wind shear stresses (τ_{wx} and τ_{wy}) at the free surface are expressed by

$$\tau_{wx} = \rho_a C_d U_{wind} \sqrt{U_{wind}^2 + V_{wind}^2} \tag{6}$$

$$\tau_{wy} = \rho_a C_d V_{wind} \sqrt{U_{wind}^2 + V_{wind}^2} \tag{7}$$

where ρ_a is the air density; U_{wind} and V_{wind} are wind velocity components at 10 m elevation in x and y directions, respectively. Although the drag coefficient C_d may vary with wind speed (Koutitas and O'Connor 1980; Jin et al. 2000), for simplicity, many researchers assumed the drag coefficient was a constant on the order of 10^{-3} (Rueda and Schladow 2003). In this study, C_d was set to 1.0×10^{-3}, and this value is applicable for simulating the wind driven flow in Deep Hollow Lake in the Mississippi Delta (Chao et al 2010).

Sediment transport modeling

The governing equation for cohesive sediment transport is based on the three-dimensional mass transport equation:

$$\frac{\partial C}{\partial t} + \frac{\partial (uC)}{\partial x} + \frac{\partial (vC)}{\partial y} + \frac{\partial (w - w_s)C}{\partial z} = \frac{\partial}{\partial x}(D_x \frac{\partial C}{\partial x}) + \frac{\partial}{\partial y}(D_y \frac{\partial C}{\partial y}) + \frac{\partial}{\partial z}(D_z \frac{\partial C}{\partial z}) \tag{8}$$

in which C is the concentration of cohesive sediment; D_x, D_y and D_z are mixing coefficients in x, y and z directions, respectively; and w_s is the settling velocity.

To solve the 3D cohesive sediment transport equation (8), the boundary conditions at the free surface and bottom are needed. At the free surface, the vertical sediment flux is zero and the following condition is applied:

$$w_s C + D_z \frac{\partial C}{\partial z} = 0 \tag{9}$$

At the bottom, the following condition is applied:

$$w_s C + D_z \frac{\partial C}{\partial z} = D_b - E_b \tag{10}$$

where D_b and E_b are deposition rate and erosion (resuspension) rate at bottom, respectively (kg/m^2/s).

Based on Krone (1962) and Mehta and Partheniades (1975), the deposition rate can be calculated by:

$$D_b = \begin{cases} 0 & \tau_b > \tau_{cd} \\ w_s C \left(1 - \dfrac{\tau_b}{\tau_{cd}}\right) & \tau_b \leq \tau_{cd} \end{cases} \qquad (11)$$

Erosion rate is generally expressed as Partheniades (1965)

$$E_b = \begin{cases} 0 & \tau_b < \tau_{ce} \\ M\left(\dfrac{\tau_b}{\tau_{ce}} - 1\right) & \tau_b \geq \tau_{ce} \end{cases} \qquad (12)$$

where τ_b is the bed shear stress (N/m²); τ_{cd} is the critical shear stress for deposition (N/m²); M is the erodibility coefficient relating to the sediment properties, the reported values are in the range of 0.00001 to 0.0004 kg/m²/s (van Rijn 1989); τ_{ce} is the critical shear stress for erosion (N/m²).

Total mercury modeling

In the water column, the concentration of total mercury can be expressed by the following mass transport equation:

$$\frac{\partial C_m}{\partial t} + \frac{\partial (u C_m)}{\partial x} + \frac{\partial (v C_m)}{\partial y} + \frac{\partial (w C_m)}{\partial z} = \frac{\partial}{\partial x}(E_x \frac{\partial C_m}{\partial x}) + \frac{\partial}{\partial y}(E_y \frac{\partial C_m}{\partial y}) + \frac{\partial}{\partial z}(E_z \frac{\partial C_m}{\partial z}) + \sum S_m \qquad (13)$$

in which u, v, w are the water velocity components in x, y and z directions, respectively; C_m is the concentration of the total mercury; E_x, E_y and Ez are the diffusion coefficients in x, y and z directions, respectively; ΣS_m is the effective source term of mercury, which can be calculated by:

$$\sum S_m = S_{load} + S_{decay} + S_{air-w} + S_{bed-w} + S_{sed} \qquad (14)$$

in which S_{load} is the external loads from upstream/ tributaries, etc.; S_{decay} is the sink term due to biodegradation; S_{air-w} is the exchange term at the air-water interface; S_{bed-w} is the bed release term; S_{sed} is the source term due to sediment erosion/ deposition. Those source terms can be expressed by:

$$S_{air-w} = k_a \left(\frac{C_g}{H_e} - f_d C_m\right) \qquad (15)$$

$$S_{decay} = -K_b C_m \qquad (16)$$

$$S_{Bed-w} = \frac{k_f}{D}(S_d - C_d) \qquad (17)$$

$$S_{sed} = J_e + J_d = \max(E_b - D_b, 0)\frac{S_T}{1-p'} + \min(E_b - D_b, 0)\left(\frac{f_p}{c_v}\right) C_m \qquad (18)$$

in which k_a is the overall volatilization transfer coefficient; C_g is the concentrations of total gaseous mercury in air; H_e is the Henry's constant; f_d is the fraction of total dissolved mercury; K_b is the overall degradation rate; k_f is the mass diffusion coefficient; S_d is the dissolved mercury concentration in bed sediment; C_d is the dissolved mercury concentration in water column; S_T is the total mercury concentration at bottom; E_b and D_b are the sediment erosion and deposition rates; p' is the porosity of bed sediment; f_p is the particulate mercury fraction; and c_v is the volumetric concentration of sediment in water column.

Numerical method

The numerical model was developed based on CCHE3D hydrodynamic model and water quality model (Jia et al. 2013, Chao et al. 2007, 2010). In this model, the staggered grid is adopted. The grid

system in the horizontal plane is a structured conformal mesh generated on the boundary of the computational domain. In vertical direction, either uniform or non-uniform mesh lines are employed.

The unsteady equations are solved using the time marching scheme. A second-order upwinding scheme is adopted to eliminate oscillations due to advection. In this model, a convective interpolation function is used for this purpose. This function is obtained by solving a linear and steady convection-diffusion equation analytically over a one-dimensional local element. Although there are several other upwinding schemes, such as the first order upwinding, the second order upwinding and Quick scheme, the convective interpolation function is selected in this model due to its simplicity for the implicit time marching scheme.

The velocity correction method is applied to solve the pressure and enforce mass conservation. Provisional velocities are solved first without the pressure term, and the final solution of the velocity is obtained by correcting the provisional velocities with the pressure solution. The system of the algebraic equations is solved using the Strongly Implicit Procedure (SIP) method.

Flow fields, including water elevation, velocity components, and eddy viscosity parameters were computed by CCHE3D. After getting the effective source terms, the total mercury concentration distribution can be simulated by solving pollutant transport equation (13) numerically.

(6) Potential risk assessment of mercury on fish

The MDEQ has issued fish consumption advisories for Grenada and Enid Lakes in the Yazoo River Basin as a result of elevated mercury concentrations. This study involved a statistical analysis of mercury data for Crappie (CR), Largemouth Bass (LMB), and Channel Catfish (CC) collected from Enid Lake in Northern Mississippi. Total Hg concentrations were compared between species. A mercury risk assessment for consumption of fish from the lake was also conducted using various assumption values to evaluate the effectiveness of the existing fish consumption advisories.

Exposure to MeHg via fish consumption was estimated using methods outlined by the EPA (Huggett et al 2001). The risk assessment includes calculations of intake rate, hazard index (HI), and monthly consumption limit (CR_{mm}) for both adults and children. The equations used are as follows:

$$\text{Intake (mg/kg/d)} = (CF \times IR \times EF \times ED)/ (BW \times AT) \tag{19}$$

Where CF is the mercury concentration in fish (mg/kg), IR is the ingestion rate (kg/meal), EF the exposure frequency (meals/yr), ED is the exposure duration (yr), BW is the body weight (kg) and AT is the averaging time (ED × 365d/yr). Initial calculations will use 8 oz for a fish meal (0.227 kg), 48 d/yr for 30 yr, and 70 kg body weight. Additional assessments can also be done to consider subsistence fish consumers and/or pregnant women or children.

A hazard index (HI) is a ratio of an individual's actual exposure over a time period (here, 30 years) to the reference dose established by the EPA. When HI < 1, the expected potential for toxicity is low, and the exposure is considered safe. When HI > 1, there is an elevated potential for toxicity associated with the exposure. Once HI is calculated, monthly consumption limits are calculated. The hazard index will be calculated for each fish species by dividing the intake by 1.0×10^{-4} mg/kg-d, the reference dose (RfD) for methylmercury. A calculated hazard index greater than one suggests human adverse effects would occur at the representative intake and consumption advisories are supported.

In addition to conducting the risk assessments described above, sediment, water, and fish concentrations measured in Enid Lake will be compared to historical values from Enid, other MS waterways, and the nation. If values are significantly elevated, this may suggest that atmospheric deposition is increasing in Enid Lake and should be considered in the TMDL assessment.

RESEARCH RESULTS

(1)Field measured data

In this project, two field trips were taken on March 12 and Nov. 18, 2013, and the water depth, flow velocity, water level, suspended sediment (SS) concentration and mercury concentration in water and sediment at each measured location (shown in Fig.3) were obtained. The measured data can be used to evaluate the sediment and mercury levels in the lake, and validate the results obtained using remote sensing technology and numerical model.

Upstream flow discharge and water surface elevation at lake outlet were obtained from USGS and US Army Corp of Engineers. Fig.5 shows the flow discharge and water surface elevation during a storm event that occurred in March, 2013.
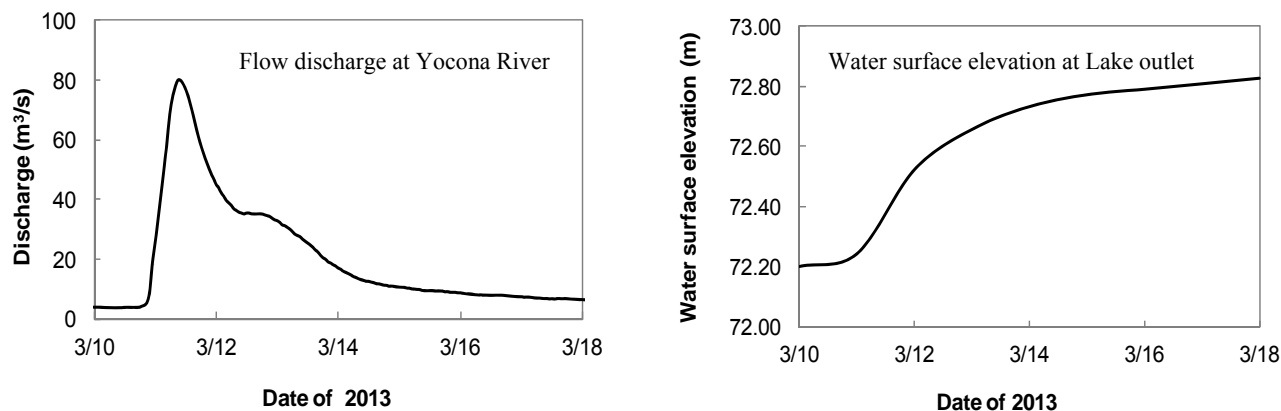

Figure 5. Flow conditions at boundary (3/10/13-3/18/13)

Wind is one of the most important driven forces for lake circulation. Fig. 6 shows the wind speed and direction near the lake.
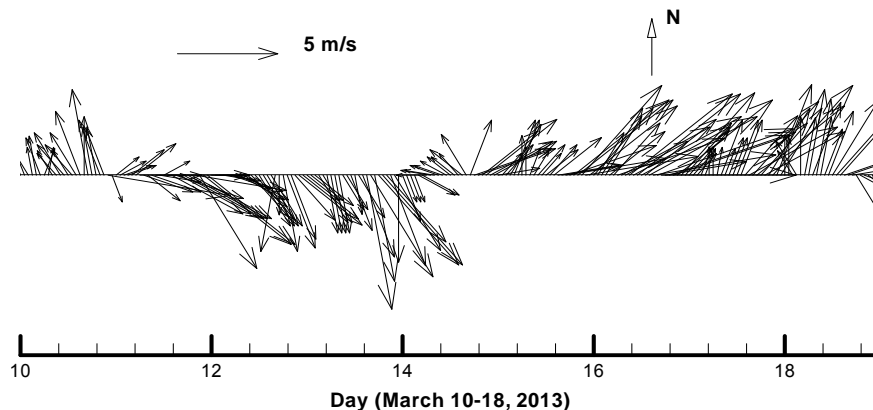

Figure 6. Wind speeds and directions near Enid Lake

Tables 1 and 2 show the measured SS and mercury data in Enid Lake.

Table 1. Mercury concentrations and water quality data for Enid Lake on 3/12/2013.

Sample Site ID	Location		T (°C)	Cl-	TDS (mg/L)	DO (mg/L)	ORP (mV)	Cond. (µs/cm)	TSS (mg/L)	K_d (L/Kg)	Total-Hg (ng/L)		PBM (ng/g)	PBM (pg/L)
	N	W									Unfiltered	Filtered		
1	34°.08.687'	89°49.033'	11.8	4.9	42.3	9.1	331.5	48.3	39.6	4.4	10.1	6.6	157	6.2
3	34°.08.552'	89°48.967'	12.3	6.7	37.7	10.3	281.6	43.8	24.3	4.3	8.1	8.4	164	6.2
4	34°.08.894'	89°49.053	12.6	10.4	42.9	9.3	313.7	50.7	60.4	4.2	8.9	7.4	125	5.8
5	34°.09.174'	89°49.054'	12.4	5.1	43.6	9.1	332.3	50.9	38.9	4.1	7.4	7.8	106	4.1
6	34°.09.469'	89°49.142	11.7	4.6	42.9	9.5	338.4	49.5	33.7	4.1	6.6	9.4	108	5.8
7	34°.09.291'	89°48.527'	12.1	4.6	43.6	9.1	341.8	50.4	48.1	4.2	7.9	7.6	124	3.2
8	34°.09.328'	89°47.855'	12.1	3.4	37.7	8.7	343.2	44.0	65.6	4.2	12.5	9.0	140	3.2
9	34°.09.358'	89°47.136'	11.8	2.5	33.2	8.3	347.5	38.3	55.2	4.1	16.3	12.3	170	7.5
10	34°.09.439'	89°46.424'	12.4	2.3	34.5	8.9	347.9	40.0	55.7	4.3	12.8	8.6	159	4.1
11	34°.09.175'	89°46.445'	11.6	2.3	33.2	9.1	347.5	38.3	44.3	4.0	14.3	14.4	135	3.6
12	34°.09.023'	89°46.961'	11.4	2.3	33.2	8.3	344.7	37.6	50.2	4.1	14.8	12.0	163	6.0
13	34°.08.816'	89°47.806'	12.6	2.8	35.1	8.3	341.3	41.4	45.2	4.6	12.7	5.3	227	9.2
14	34°.08.656'	89°50.280'	11.6	3.7	39.0	9.9	329.6	44.3	20.5	4.5	4.9	4.3	150	9.4
15	34°.08.393'	89°51.268'	11.1	3.7	37.7	9.7	332.1	42.4	15.2	4.8	6.0	3.9	224	8.9
16	34°.08.594'	89°51.663'	10.7	3.9	37.7	9.7	330.1	42.5	11.7	4.7	5.9	4.5	224	6.0
17	34°.09.246'	89°51.662'	10.6	3.9	38.4	9.7	330.1	43.0	14.6	4.6	5.8	4.6	201	8.2
18	34°.09.700'	89°50.657'	10.5	4.3	39.7	9.5	322.9	44.0	14.3	4.6	8.0	4.2	170	10.3
19	34°.09.580'	89°49.644'	11.1	5.0	40.3	9.2	272.5	45.3	8.6	5.0	6.2	3.8	371	3.1
Mean			11.7	4.2	38.5	9.2	329.4	44.2	35.9	4.4	9.4	7.5	173.1	3.4
Median			11.8	3.9	38.0	9.2	332.2	43.9	39.3	4.3	8.1	7.5	160.9	2.6
SD			0.7	1.9	3.6	0.6	21.2	4.3	18.5	0.3	3.6	3.2	61.8	2.9
Min			10.5	2.3	33.2	8.3	272.5	37.6	8.6	4.0	4.9	3.8	106.5	2.4
Max			12.6	10.4	43.6	10.3	347.9	50.9	65.6	5.0	16.3	14.4	370.6	3.2

Table 2. Mercury concentrations and water quality data for Enid Lake on 11/18/2013

Sample Site ID	GPS Coordinates	Water Depth (m)	Temp. (°C)	Cl (mg/L)	TDS (mg/L)	DO (mg/L)	Cond. (μs/cm)	ORP (mV)	TSS (mg/L) Lab Data	TSS (mg/L) Field Probe	Mercury (ng/L) Unfiltered	Mercury (ng/L) Filtered
1	N 34 09.096 W089 48.306	1.3	11.0	6.8	93.0	8.2	110.6	-126.3	58.0	48.3	11.24	5.8
2	N 34 08.767 W089 48.278	1.0	10.3	5.8	97.5	8.4	112.3	-98.7	66.0	68.7	22.59	3.3
3	N 34 08.720 W089 48.793	1.3	11.5	6.3	95.6	8.3	112.8	-135.2	67.6	71.0	41.92	18.7
4	N 34 08.720 W089 48.379	2.3	12.0	8.0	98.2	8.1	117.7	-138.9	74.0	75.7	6.29	3.8
5	N 34 08.784 W089 49.915	2.7	11.5	8.7	96.4	8.5	115.1	-138.9	53.2	39.7	9.21	48.1
6	N 34 09.132 W089 48.826	1.8	11.5	6.6	93.0	9.0	110.2	-112.1	34.4	31.3	6.41	4.8
7	N 34 09.471 W089 48.843	0.8	11.0	6.5	92.7	9.0	109.6	-92.1	31.6	25.3	5.26	3.1
8	N 34 09.586 W089 49.366	1.1	11.2	6.2	92.5	9.1	109.7	-120.0	47.6	38.7	10.02	3.0
9	N 34 09.22 W089 49.371	2.5	11.5	7.3	92.3	9.2	110.0	-119.3	33.6	19.7	7.53	7.1
10	N 34 09.245 W089 49.932	3.4	12.5	7.6	93.4	8.9	111.5	-115.7	25.6	16.7	5.37	3.7
11	N 34 09.587 W089 49.968	1.1	11.5	7.7	93.4	9.2	109.3	-112.5	41.6	30.0	9.29	4.3
12	N 34 09.59 W089 50.451	2.7	12.5	8.5	93.6	9.1	111.8	-98.2	28.8	19.0	5.19	7.6
13	N 34 09.254 W089 50.443	3.7	12.0	8.1	93.6	9.3	112.0	-111.5	21.2	15.0	6.56	7.3
14	N 34 08.799 W089 50.433	3.9	11.5	8.3	92.5	9.3	110.7	-90.7	29.6	19.3	7.16	4.9
15	N 34 08.354 W089 50.508	1.4	11.5	10.0	106.6	9.0	128.8	-124.5	68.8	66.3	8.33	4.3
16	N 34 08.186 W089 50.526	0.6	11.5	8.7	110.3	9.4	132.7	-93.5	82.0	74.7	6.30	9.1
17	N 34 08.805 W089 50.990	3.7	11.5	8.8	92.1	9.5	110.1	-128.4	29.2	15.3	6.58	32.5
18	N 34 09.264 W089 50.984	4.2	11.5	9.6	92.5	9.4	110.8	-136.8	19.2	14.0	4.07	8.6
19	N 34 09.232 W089 51.547	4.3	11.5	8.5	93.2	9.3	111.8	-119.4	16.8	17.0	4.50	7.5
20	N 34 09.226 W089 52.094	4.4	11.0	7.9	92.3	9.0	110.1	-125.8	20.4	19.3	4.57	22.3
21	N 34 08.771 W089 52.093	4.5	11.3	7.8	92.3	9.2	110.2	-109.9	14.4	15.0	3.96	4.2
22	N 34 08.469 W089 52.126	1.0	11.0	8.2	93.4	9.7	111.4	-129.3	40.0	29.7	6.35	11.4
23	N 34 08.457 W089 53.165	1.6	11.0	8.0	92.3	9.7	110.1	-117.8	26.0	19.3	7.25	6.7
24	N 34 08.811 W089 53.136	2.3	11.0	9.1	92.3	9.4	110.3	-132.9	12.0	15.7	7.85	36.3
25	N 34 08.216 W089 53.666	2.0	11.0	9.7	92.3	10.1	107.6	-137.0	27.2	22.3	6.33	13.6
26	N 34 08.51 W089 54.079	0.8	11.0	8.1	91.7	10.5	106.8	-93.6	33.2	21.7	7.76	19.9
27	N 34 08.938 W089 54.18	6.7	10.7	8.9	91.7	9.5	109.2	-134.7	19.6	14.3	6.92	8.6
28	N 34 09.399 W089 54.09	5.7	10.5	9.3	91.0	9.3	108.6	-128.6	20.4	10.3	5.10	11.0
29	N 34 09.815 W089 53.027	2.1	10.7	9.8	93.4	9.3	110.3	-139.6	24.0	20.3	4.55	24.1
30	N 34 09.223 W089 53.182	5.2	11.0	8.1	92.3	9.2	110.2	-130.9	16.4	16.0	3.82	2.2
31	N 34 12.25 W089 40.733	<1	11.0	19.4	123.1	10.2	137.1	-141.6	8.8	2.3	26.68	5.8

On 11/18/2013, flow velocities in the lake were measured using ADCP by scientists at NSL. At each sampling location (Fig. 3b), the *u* and *v* velocities were measured from near surface to the near bottom. The field measurements can be used to calibrate the numerical model results.
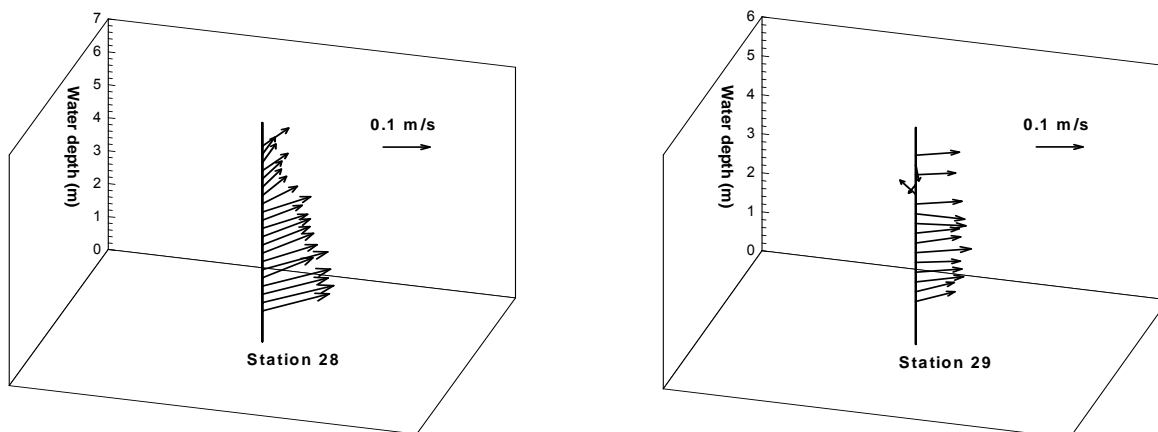

Figure 7. Measured velocity fields in the lake (11/19/2013)

(2) Remote sensing based suspended sediments and associated mercury concentration estimation

Several studies had success in estimating TSS using simple linear regression techniques involving MODIS VNIR bands and in situ measurements (e.g., Richard et al., 2004; Wang et al., 2009). A similar approach was used in this study to estimate TSS in Enid Lake. The correlation coefficient of the regression equation was obtained using near-real time in situ measurements of total suspended sediments and the reflectance values of the red (R) and near infra-red (NIR) bands of the Moderate-resolution Imaging Spectroradiometer (MODIS) (Band 1 and Band 2) imagery acquired on March 12, 2013 and November 20, 2013. The March and November datasets include 18 and 30 in situ measurements, respectively. The concentration of mercury (unfiltered) in the obtained suspended sediment samples was measured and correlated with the MODIS reflectance values for the corresponding samples.

Fig.8 shows the correlation between MODIS Reflectance of R and NIR Bands (Band 1 and Band 2) and TSS respectively for March 12, 2013. Fig. 9 shows the correlation between MODIS Reflectance of R and NIR Band (Band 1 and Band 2) and Total Hg (Unfiltered) for March 12, 2013.
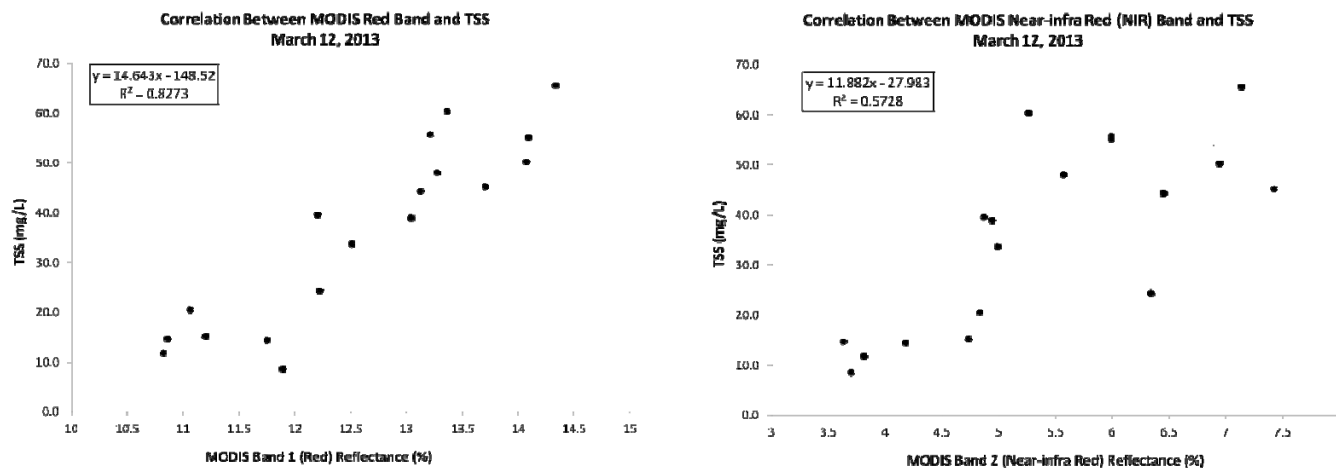

Figure 8. The correlation between MODIS Reflectance of R and NIR Bands (Band 1 and Band 2) and TSS respectively for March 12, 2013.
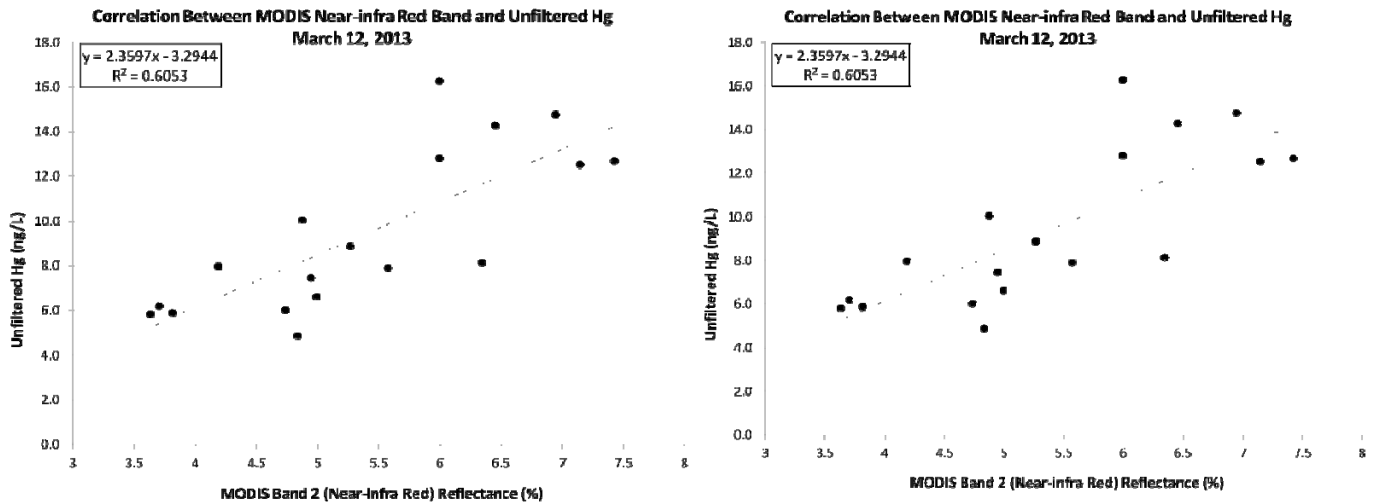
Figure 9. The correlation between MODIS Reflectance of R and NIR Band (Band 1 and Band 2) and Total Hg (Unfiltered) for March 12, 2013.

The obtained regression equations were applied on the water pixels of the MODIS NIR imagery to estimate the suspended sediments and associated mercury concentrations in the lake at 250 m spatial resolution. These 250 m resolution measurements were then used to interpolate 1 m resolution estimation of suspended sediments and associated mercury in the lake water. Fig.10 shows the distribution of the estimated SS. It can be found, the SS concentration cannot be determined in some areas where the water depth is very shallow using the remote sensing technology. Fig. 11 shows the distribution of the estimated suspended sediments associated with mercury concentration in the lake water.
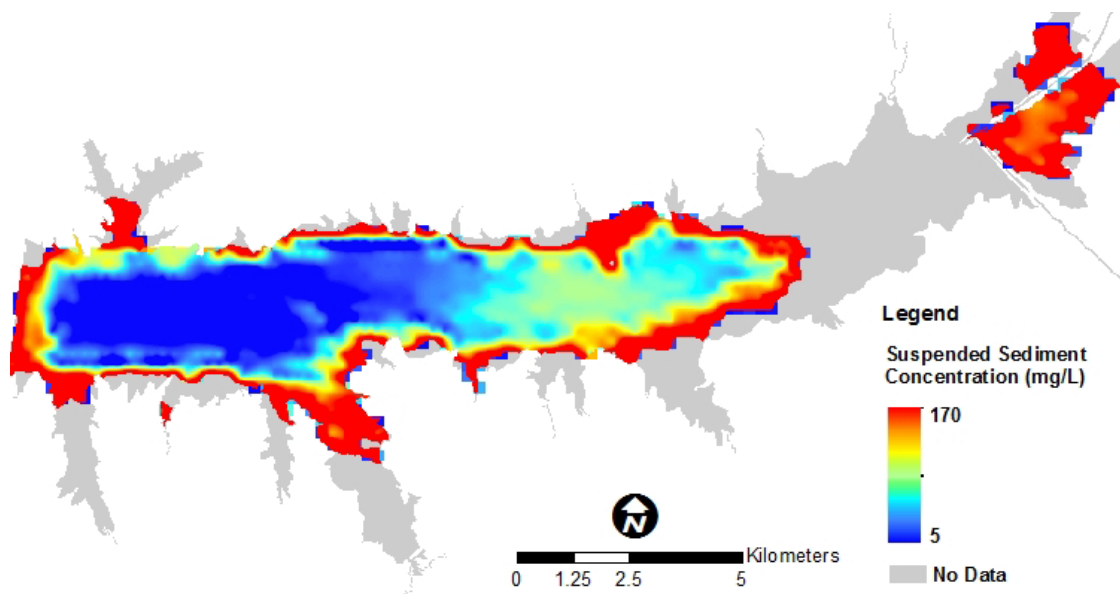
Figure 10. Distribution of SS in Enid Lake estimated by MODIS imagery acquired on March 12, 2013.
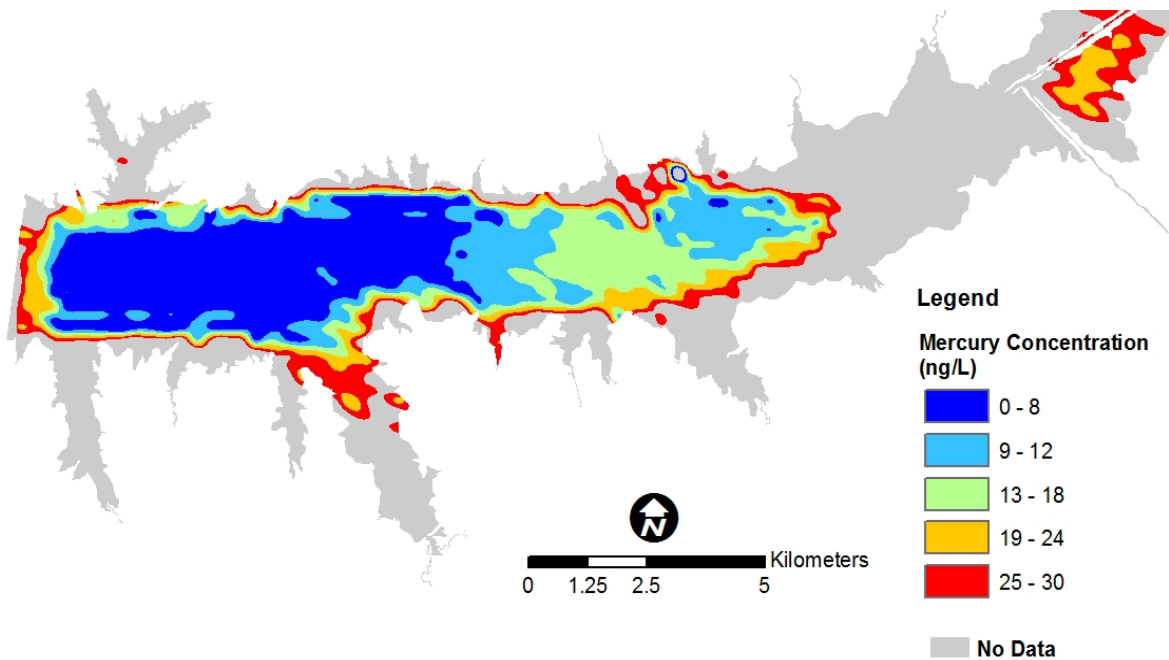
Figure 11. Distribution of total mercury concentration in SS of Enid Lake estimated by MODIS imagery acquired on March 12, 2013.

(3) Numerical model results

Based on initial bed elevation data (Fig. 12), the computational domain was discretized into a structured finite element mesh using the CCHE Mesh Generator. In the horizontal plane, the computational domain was represented by a mesh with 353×171 nodes. In the vertical direction, the domain was divided into 8 uniform layers. A simulation period from March 10 to 18, 2013, was selected for model test. After obtaining the boundary conditions shown in Fig. 5, the developed model can be applied to simulate the flow, SS and mercury distributions in the lake.

Fig. 13 shows the flow velocities on the water surface and near the bed, which was induced by the upstream river discharge as well as the wind forces.
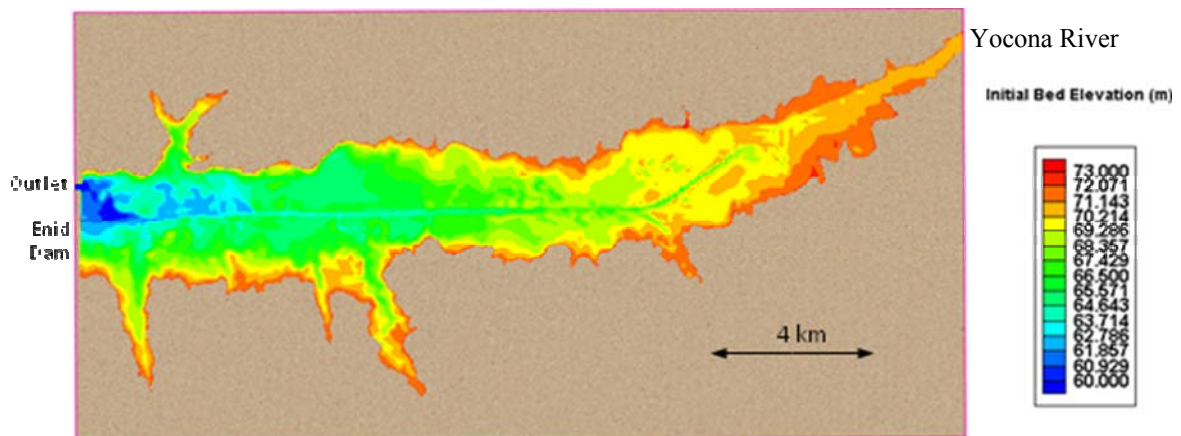

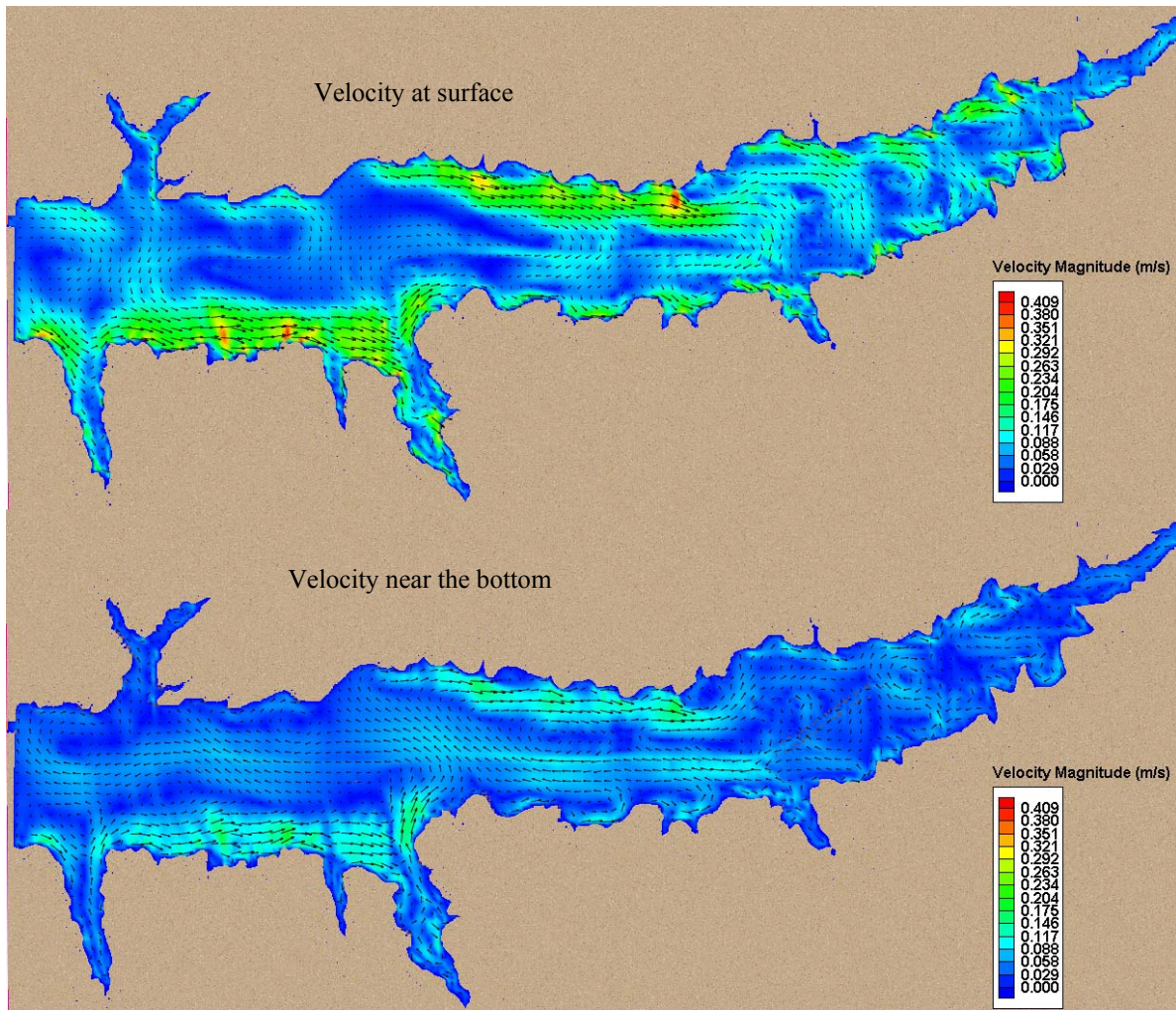Figure 12. Initial bed elevation of Enid Lake

Figure 13. Simulated flow patterns in Enid Lake

Fig. 14 shows the simulated concentration of SS in the lake on March 12, 2013. It is generally in good agreement with the results obtained based on remote sensing technology (Fig. 10). The SS concentrations were higher near the river mouth and shoreline area, while the concentration of SS was much lower in the deeper water near the dam. Some differences between numerical results and remote sensing data can be observed near northwest shoreline. The numerical model underestimates the SS concentration in this area. It may be the reason that the effect of wind induced wave on the sediment resuspension was not taken into account in the numerical model.
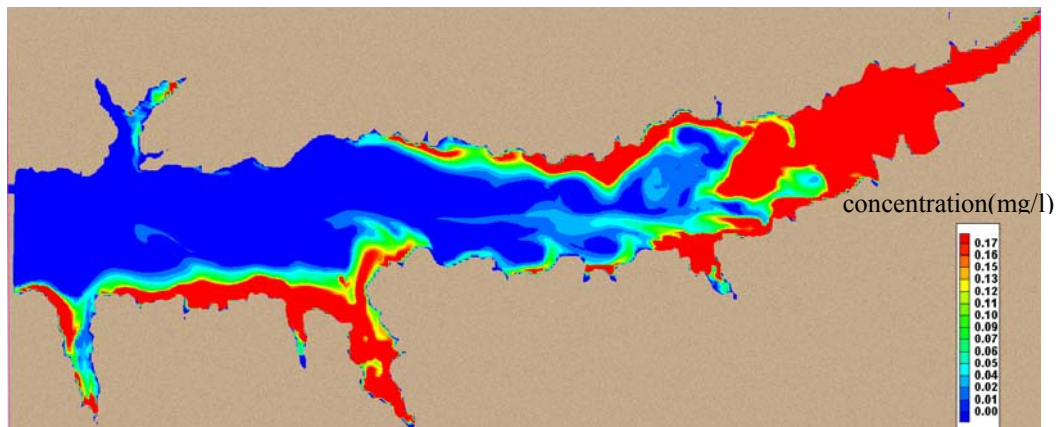

Figure 14. Simulated concentration of SS in Enid Lake (compared with Fig. 10)

Fig. 15 shows the simulated concentration of total mercury in the lake on March 12, 2013. It is generally in good agreement with the results obtained based on remote sensing technology (Fig. 11). Some differences between numerical results and remote sensing data can be observed near northwest shoreline. It may be the reason that the numerical model underestimated the SS concentration in these areas. So the concentration of sorbed mercury on the sediment was also underestimated by the numerical model.
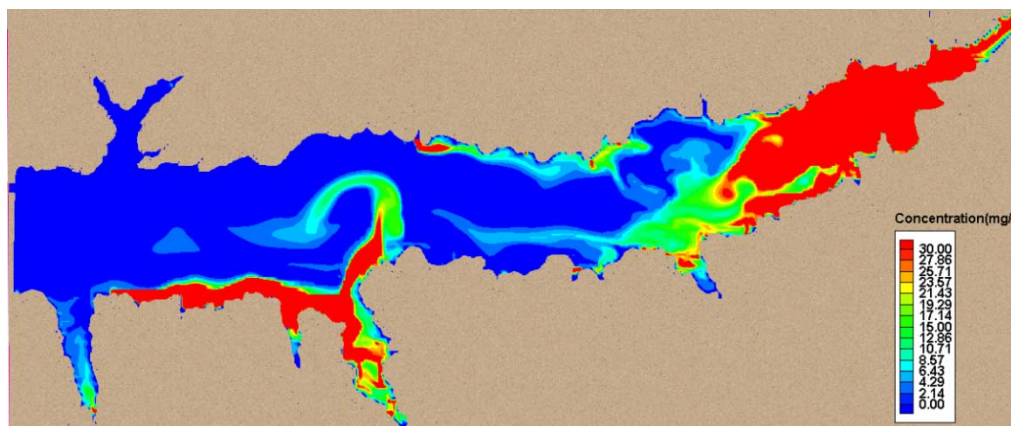

Figure 15. Simulated total mercury concentration in Enid Lake (compared with Fig. 11)

(4) Risk assessment of mercury on fish

Linear regression analysis of length vs. weight suggested that LMB and CC exhibited similar growth trends. The relationship between length and weight for CR from Enid Lake was statistically different from that of CR from other lakes, suggesting that environmental factors unique to Enid Lake may affect the growth of CR there.

Of the fish analyzed, LMB consistently had the highest mean mercury concentrations (in mean ± SE, 386 ± 76 ng/g), followed by CC (152 ± 14 ng/g) and then CR (214 ± 10 ng/g) (shown in Table 3). The average Hg concentration in LMB exceeded the threshold concentration of 300 ng/g that is enforced by the EPA.

Table 3. Mean mercury concentrations for CR, LMB, and CC in Enid Lake (red represents Hg exceeding the EPA standard (300 ng/g). Blue exceeds MDEQ value (750 ng/g), n=number of fish).

Lake	Enid Lake		
Hg (ng/g)	CR n=16	LMB n=9	CC n=14
Mean	214	386	152
Standard Error (1 SE)	10	76	14
Min	120	184	84
Max	285	954	272
Median	215	344	146

Linear regression analysis of length vs. Hg concentration showed that only LMB have a strong relationship between length and Hg concentration. Because the existing fish consumption advisories are length-based, the lack of relationship between length and Hg concentration means they may be insufficient to protect the public from exposure to MeHg.

Seven variations of risk assessment calculations yielded hazard index (HI) and monthly consumption limit (MCL) values that further discredit the existing consumption advisories and many consumption recommendations (Table 4). In four of the seven methods ("Hugget", "Ingestion Rate 15 lbs/person/year", "Body Weight (Portier 2007)" and "Body Weight (EPA 2011)"), LMB from Enid Lake had an adult HI>1.

All fish species from the lake yielded HI>1 for children.

Table 4. Comparison of Mean HI (Hazard Index) and MCL (Mean Consumption Limit in meals/month) for each set of risk assessment assumptions (red: above EPA's standard of HI = 1).

Risk Assessment Method			Species		
			CR	LMB	CC
Hugget	Mean HI	Adult	0.91	1.6	0.65
		Child	4.4	8.0	3.1
	MCL	Adult	4.5	3	7
		Child	1	0.5	1.5
Ingestion Rate (15 lbs/person/year)	Mean HI	Adult	0.57	1.0	0.41
		Child	2.8	5.0	2.0
	MCL	Adult	7.5	5	11
		Child	1.5	1	2.5
Ingestion Rate (3 oz/meal)	Mean HI	Adult	0.34	0.62	0.24
		Child	1.7	3.0	1.2
	MCL	Adult	12	8	18
		Child	2.5	1.5	4
Consumption Frequency	Mean HI	Adult	0.46	0.82	0.33
		Child	2.2	4.0	1.6
	MCL	Adult	4.5	3	7
		Child	1	0.5	1.5
Body Weight (Portier 2007)	Mean HI	Adult	0.85	1.5	0.61
		Child	3.8	6.8	2.7
	MCL	Adult	5	3	7.5
		Child	1	0.5	1.5
Body Weight (EPA 2011)	Mean HI	Adult	0.80	1.4	0.57
		Child	4.0	7.2	2.8
	MCL	Adult	5	3.5	8
		Child	1	0.5	1.5
Ingestion Rate & Body Weight (EPA 2001)	Mean HI	Adult	0.50	0.90	0.36
		Child	2.2	4.5	1.8
	MCL	Adult	8	5.5	12.5
		Child	1.5	1	2.5

DISCUSSION

The transport, fate and risk of mercury in Enid Lake have been studied based on field observation, laboratory measurement, remote sensing technology, numerical model, and risk assessment. This

study indicates that the major sources of mercury in Enid Lake include river inflow from Yocona River, and runoff from surrounding watersheds. It has been observed that the mercury are generally bounded with sediment and introduced to the lake due to the transport of sediments (Garry 2013). The movement of sediment and deposition/erosion processes are greatly affect the distribution of mercury in the lake.

Measured Hg and water quality data showed there were differences between the sites nearer the dam (e.g., sites 15, 16, 17) and those closer to the Yocona River (e.g., sites 9, 10, 11, 12). The deeper water near the dam tended to be cooler, with higher dissolved oxygen, and slightly higher total dissolved solids and conductivity. However, the biggest difference was total suspended solids, which averaged 13.6 ± 1.9 mg/L near the dam and 48.9 ± 5.3 ng/L away from the dam (for the spring storm). This likely reflects the deposition (loss) of particles as the water slows as it traverses the lake. This gradients in TSS and Hg were also observed in satellite imagery and numerical model results.

For the spring event, concentrations of Hg averaged 9.4 ± 3.6 ng/L (1 SD, n=18) and ranged from 4.9 to 16.3 ng/L for unfiltered water; Hg in the dissolved fraction (<0.45 μm) averaged 7.5 ± 3.2 ng/L and ranged from 3.8 to 14.4 ng/L. Mercury concentration was correlated with TSS (r=0.683, p<0.05). Concentrations in the sediment averaged 65.2 ng/g, and ranged from 40.7 to 89.7 ng/g. The bulk of the sediment (>80%) consisted of particles <125 μm in diameter. Concentrations of Hg in these fines were greater than the larger size fractions, not surprising given that Hg^{+2} is surface reactive. Mercury also has an affinity for organic matter. Indeed levels of Hg and organic matter were higher in the sediment from the more shallow part of the lake near the mouth of the Yocona River compared to the deeper water areas near the dam.

Remote sensing technology has been successfully used to estimate and map the distributions of SS and mercury on the entire lake surface following a storm event. It also provided useful information for numerical model calibration and validation. Overall, this study shows that suspended sediment particle size, organic matter, and water flow characteristics are important factors controlling the distribution of Hg in the lake, and that modeling suspended solids and Hg transport using spectral data acquired remotely by satellites is not only feasible but a powerful way to provide timely data on the dynamics of Hg in reservoirs. Moreover, the results from this study are directly applicable to other large lake systems in Mississippi and elsewhere.

A numerical model has been developed to predict the dynamic flow fields, and the temporal and spatial concentrations of sediment and mercury in the entire lake. Based on the upstream river flow discharge, download water surface elevation, and wind conditions, the flow fields, including velocity, water level, eddy viscosity, etc. can be solved. After obtaining flow information, the model can be applied to simulate the concentrations of SS and mercury in the lake. The developed model was used to simulate a spring storm event and the modeling results of SS and Hg were generally in good agreement with satellite imagery. In general, the concentrations of SS and Hg were higher near the river mouth and shallow shoreline area than that in the deeper water areas near the dam. The model provides a useful tool to predict the long time trend of mercury in the lake.

Risk assessment analysis shows that the mercury concentration in LMB collected from Enid Lake exceed the maximum concentrations allowed by the EPA (300 ng/g). Compared with the data collected by Hugget (1999), Hg in all fish species in Enid Lake have decreased, likely as a result of MDEQ recently refocused efforts to locate possible sources of mercury and monitor water quality (MDEQ 2012). For Hazard Index, all fish species from Enid Lake yielded HI>1 for children. CR and CC from the lake had an HI<1 for adult. In four of the seven methods ("Hugget", "Ingestion Rate 15 lbs/person/year", "Body Weight (Portier 2007)" and "Body Weight (EPA 2011)"), LMB from Enid Lake had an adult HI>1.

SIGNIFICANT FINDINGS

- The major sources of mercury in Enid Lake include river inflow from Yocona River, runoff from surrounding watersheds, and atmospheric deposition.
- Mercury concentration can be measured in both water and sediment samples.
- Mercury is generally absorbed on sediment and introduced to the lake due to the transport of sediments.
- Remote sensing technology can be used to estimate the concentrations of SS and Hg on the entire lake surface.
- Numerical model is an effective tool to predict the dynamic flow fields, and the temporal and spatial concentrations of sediment and mercury and in large lakes.
- In Enid Lake, the concentrations of SS and Hg are generally higher near the Yocona River mouth and shallow shoreline area compared to the deeper water areas near the dam.
- The measured data shows that the Hg concentration in LBM from Enid Lake exceed the maximum concentration of 300 ng/g allowed by the EPA.
- Hg level in all fish species in Enid Lake have decreased compared to the data obtained 10 years ago.
- All fish species from Enid Lake yielded HI>1 for children, which means there is an elevated potential for toxicity associated with the exposure. For CR and CC, HI was less than 1 for adult, and the expected potential for toxicity was low. For LMB, among seven risk assessment methods, results from four methods show LMB from Enid Lake had an adult HI>1.

FUTURE RESEARCH

In this project, the proposed research tasks have been successfully studied. Due to the limitations of funds and time, we could not address all the questions we found during the project period. They might be interesting topics for our future research.

Although we have obtained the general distributions of sediment and associated mercury concentration in the lake, the amount of mercury absorbed on the suspended sediment or deposited to the lake bottom is still a question to be answered to assess the mercury mass balance in the lake. This can be achieved by understanding the mercury sedimentation processes, such as adsorption/desorption of mercury by sediment and mercury release from bottom sediment.

In Yazoo River Basin, spring and fall are the major raining seasons. A large amount of sediment is discharged into Enid Lake due to storm events, resulting in high level mercury introduced into the lake and greatly affect the mercury concentration in the lake, as well as in the fish. Although we have obtained the sediment and mercury distributions during a storm event, to understand the amount of mercury deposited to the lake, the long term historic storm events and associated sediment/mercury transport need to be studied.

The impact of the mercury released from the bottom sediment is critical for proper risk assessment of mercury for the lake. In addition to the understanding of the fate and transport of mercury in Enid Lake, it is also important to provide useful information about the mercury concentrations in water, suspended sediment, bottom sediment, and fish tissue, which are directly relevant to stakeholders concerned with wildlife and human consumption of mercury.

STUDENT TRAINING

Stacy Wolff graduated from the University of Mississippi's Honors College with a Bachelor of Science Degree in Forensic Chemistry. Her thesis was titled "Mercury in fish in north Mississippi reservoirs: statistical analysis and risk assessment". She was involved in the water and fish analyses.

Garry Brown, who graduated with a Ph.D. in Analytical Chemistry in August 2013, made significant contributions to this work. His dissertation was titled "Studies of mercury in water, sediment, and fish in Mississippi: concentrations, speciation, cycling, and isotopic composition".

Sara Adams, a summer 2013 REU (research experience for undergraduates) student, was also involved in the fish analyses.

Derek Bussan, a graduate student in chemistry, helped with the field work.

ACKNOWLEDGEMENTS

REFERENCES

Bennet, S.J. and Rhoton, F.E. (2009). Linking upstream channel instability to downstream degradation: Grenada Lake and the Skuna and Yalobusha River Basin, Mississippi, Ecohydrology, Vol. 2, 235-247.

Binding, C. E., Bowers, E.G., and Mitchelson-Jacob. 2005. Estimating suspended sediment concentrations from ocean color measurements in moderately turbid waters; the impact of variable particle scattering properties. Remote Sensing of Environment. 94(2005):373-383.

Chao, X., Jia, Y. , Cooper, C., Shields, D. and Wang, S.S.Y.(2006), Development and Application of a Phosphorus Model for a Shallow Oxbow Lake, Journal of Environmental Engineering, 132, No. 11, 1498-1507.

Chao, X., Jia, Y.F., Shields, D., Wang, S.S.Y. and Cooper, C.(2007). "Numerical Modeling of Water Quality and Sediment Related Processes", Ecological Modelling, Vol. 201, 385-397.

Chao, X., Jia, Y., Shields, F. D. Jr., and Wang, S.S.Y. (2008), Three-dimensional numerical modeling of cohesive sediment transport and wind-wave impact in a shallow oxbow lake, Advances in Water Resources, 31, 1004-1014.

Chao, X., Jia, Y., Shields, F. D. Jr., Wang, S.S.Y. and Charles M. Cooper (2010), Three-Dimensional Numerical Modeling of Water Quality and Sediment-Associated Processes with Application to a Mississippi Delta Lake, Journal of Environmental Management, 91(7), 1456-1466.

Grandjean,P., Satoh,H., Murata,K. and Eto,K., (2010). Adverse effects of methylmercury: environmental health research implications. Environ Health Perspect. 118, 1137-1145.

Hossain, A., Jia, Y., and Chao, X., 2010, Development of Remote Sensing Based Index for Estimating/Mapping Suspended Sediment Concentration in River and Lake Environments, Proceedings of 8th International Symposium on ECOHYDRAULICS (ISE 2010), September 12-16, 2010, COEX, Seoul, Republic of Korea, Paper No. 0435, pp. 578-585.

Huggett, D.B., Steevensa, J.A., Allgoodb, J.C., Lutkenc, C.B., Gracec, C.A., and Benson, W.H. (2001). Mercury in sediment and fish from North Mississippi Lakes, Chemosphere, 42, 923-929.

Jia, Y., Scott, S., Xu, Y., Huang, S., and Wang, S. S. Y. (2005). Three-dimensional numerical simulation and analysis of flows around a submerged weir in a channel bendway, J. Hydraul. Eng., 131(8), 682–693

Jia, Y., Scott, S., Xu, Y., and Wang, S. S. Y. (2009). Numerical Study of Flow Affected by Bendway Weirs in Victoria Bendway, the Mississippi River, J. Hydraul. Eng., 135(11), 902-916.

Jia, Y., Chao, X., Zhu, T. (2013), Technical Manual of CCHE3D, Version1.0, NCCHE-TR-01-2013.

Karagas,M.R., Choi,A.L., Oken,E., Horvat,M., Schoeny,R., Kamai,E., Cowell,W., Grandjean,P. and Korrick,S., (2012). Evidence on the human health effects of low-level methylmercury exposure. Environ Health Perspect. 120, 799-806.

Katsenovich, Y., Tachiev, G., Fuentes, H.R., Roelant, D. and Henao, A. (2010), A study of the mercury sorption and transport with Oak Ridge Reservation soil, 2010 Waste Management Conference, March 7-11, Phoenix, AZ.

Knightes,C.D., Sunderland,E.M., Craig,B.M., Johnston,J.M. and Ambrose,R.B., (2009). Application of ecosystem-scale fate and bioaccumulation models to predict fish mercury response times to changes in atmospheric deposition. Environ Toxicol Chem. 28, 881-893.

Koutitas, C., and O'Connor, B., (1980). Modeling three-dimensional wind-induced flows. ASCE, Journal of Hydraulic Division, 106 (11), 1843-1865.

Krone, R.B. 1962. Flume Studies on the Transport of Sediment in Estuarine Shoaling Processes, Hydraulic Engineering Laboratory, University of California, Berkeley.

Kuwabara, J.S. et al. (2003), Sediment-water interactions affecting dissolved-mercury distributions in Camp Far West Reservoir, California, USGS, Water Resources Investigations Report 03-4140

Lathrop R G. 1992. Landsat Thematic Mapper monitoring of turbid inland water quality. Photogramm. Eng. Remote Sens. 58(4): 465-470.

MDEQ (2002). Yocona River and Enid Reservoir Phase One Total Maximum Daily Load For Mercury, TMDL/WLA Branch, Mississippi Department of Environmental, Jackson, MS.

MDEQ (2010). State of Mississippi Water Quality Assessment 2010 Section 305(b) Report, Office of Pollution Control, Mississippi Department of Environmental, Jackson, MS.

MDEQ (2012). State of Mississippi Water Quality Assessment 2012 Section 305(b) Report, Office of Pollution Control, Mississippi Department of Environmental, Jackson, MS.

Partheniades, E.(1965). Erosion and deposition of cohesive soils. J. Hydraulic Division, ASCE, 91(HY1).

Populus, J., Hastuti, W., and Martin, J. L. 1995. Remote sensing as a tool for diagnosis of water quality in Indonesian Seas. Ocean & Coastal Management. 27(3): 197-215.

Portier, K., Tolson, J. K., & Roberts, S. M. (2007). Body weight distributions for risk assessment. Risk Analysis,27(1), 11-26.

Rueda FJ, Schladow SG. 2003. Dynamics of large polymictic lake. II: Numerical Simulations. Journal of Hydraulic Engineering. 129(2): 92-101.

Selin,N.E., Sunderland,E.M., Knightes,C.D. and Mason,R.P., (2010). Sources of mercury exposure for U.S. seafood consumers: implications for policy. Environ Health Perspect. 118, 137-143.

United States Environmental Protection Agency. (2011). Body weight studies. In United States Environmental Protection Agency (Ed.), EPA Exposure Factors Handbook.

Van Rijn, L. C. (1989). Handbook Sediment Transport by Currents and Waves, Report H461, Delft Hydraulics.

Wang, S.S.Y., Roche, P.J., Schmalz, R.A., Jia, Y., and Smith, P.E. (ed.) 2008, Verification and Validation of 3D Free-Surface Flow Models, American Society of Civil Engineering, Reston, Virginia.

Wang, X., Wang, Q., and Wu, Q. 2003. Estimating suspended sediment concentration in coastal water of Minjiang River using remote sensing images. Journal of Remote Sensing. 7(1): 54-57.

Ward,D.M., Nislow,K.H. and Folt,C.L., 2010. Bioaccumulation syndrome: identifying factors that make some stream food webs prone to elevated mercury bioaccumulation. Ann N Y Acad Sci. 1195, 62-83.

Williams, A. N., and Grabau, W. E. 1973. Sediment concentration mapping in tidal estuaries. In Third Earth Resources Technology Satellite-1 Sym. NASA SP-351, 1347-1386.